Zeeman Effects in the Edge Emission and Absorption of ZnO

D. C. Reynolds, C. W. Litton, and T. C. Collins
Aerospace Research Laboratories, Wright-Patterson Air Force Base, Ohio
(Received 28 June 1965)

Of the more than 20 sharp characteristic emission and absorption lines observed in the edge emission and absorption spectra of ZnO platelets, several typical lines have been examined in detail experimentally at low temperatures (~1°K). Zeeman effects, in magnetic fields up to 45 000 G, have been studied in singlets as well as zero-field-split doublets. In particular, the magnetic splitting of I_9 (an emission line appearing at 3692.64 Å) has been studied as a function of magnetic field orientation (angular orientation of c axis with respect to field direction). In accordance with the Thomas-Hopfield theory, arguments have been presented for the association of I_9 with a bound-exciton complex; this line has been observed to split linearly as a function of field strength, and an isotropic electron g value of -1.93 has been determined at $C\perp\mathbf{H}$. The line I_9 is further characterized by an anisotropic hole g value which has been determined to be -1.24 at $C\|\mathbf{H}$. A zero-field-split fluorescent doublet, I_2-I_3 (3680.63, 3681.59 Å), which splits nonlinearly as a function of field strength, has been studied as a function of field orientation. The I_2-I_3 doublet has been attributed to an ionized exciton complex, and effective electron and hole g values have been determined. Electron g values are isotropic and essentially the same for all of the lines (about -1.95), while the hole g value is not only anisotropic for each line, but also assumes different values in the different complexes (lines), indicating that the hole is sensitive to its state of binding in the exciton complex.

INTRODUCTION

ZINC oxide, known since the time of the ancients, occurs naturally as the mineral zincite and has been the subject of extensive investigation for many years. In fact, over a period of more than 25 years, many of the electrical and optical properties of ZnO crystals (of both natural and synthetic origin) have been measured, a summary of which is given in the excellent review by Heiland, Mollwo, and Stockmann[1]; however, it has only been during the past ten years that both the semiconducting and optical properties of ZnO have received what one might call quantitative treatment. Although Beutel and Kutzelnigg[2] were among the first to discover that ZnO could be excited to luminescence, a fairly detailed measurement of the ZnO edge fluorescence spectrum has only recently been made by Andress and Mollwo[3] and by Andress[4]; also, a detailed study of the reflection and absorption spectra near the onset of intrinsic absorption has only recently been made by Thomas *et al.*[5,6] ZnO, like several of the other II–VI compounds, crystallizes in the hexagonal modification or wurtzite structure. The first analysis of the wurtzite structure in terms of an energy-band scheme (band extrema at $\mathbf{k}=0$ or Γ symmetry point) was made by Birman.[7]

Assuming a tight-binding approximation, in conjunction with group theory, Birman[7] arrived at the irreducible representations, band symmetries, and optical selection rules for both the zincblende and the wurtzite structures. In this approximation (sometimes called linear combination of atomic orbitals), the upper valence-band states are made up of the p states of the anion; hence, the valence-band states are constructed from approximate linear combinations of products of P_x, P_y, and P_z hydrogen-like orbitals, including electron spin. Similarly, the lowest conduction-band states are made up of the s states of the cation. In the absence of both spin-orbit and crystalline-field interactions, the P states are degenerate. The uniaxial crystalline field of the wurtzite lattice partially lifts this degeneracy, separating the P_z from the P_x, P_y orbitals. Finally, the P_x, P_y, and P_z bands are split into a Γ_9 band and two Γ_7 bands by spin-orbit coupling. This p-like structure at $\mathbf{k}=0$, along with the band sym-

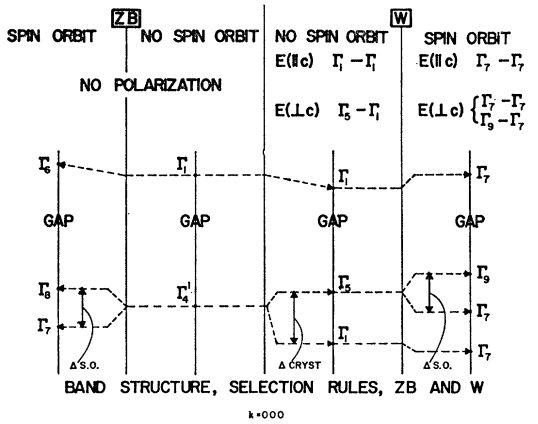

FIG. 1. Band structure and selection rules for zincblende and wurtzite structures at the Γ symmetry point ($\mathbf{k}=0$). Crystal splittings and spin-orbit splittings are indicated schematically. Transitions which are allowed for various polarizations of photon electric vector with respect to the crystalline "C" axis are indicated, i.e., $\mathbf{E}\perp C$ or $\mathbf{E}\|C$. (After Birman.)

[1] G. Heiland, E. Mollwo, and F. Stockmann, in *Solid State Physics*, edited by F. Seitz and D. Turnbull (Academic Press Inc., New York, 1959), Vol. 8.
[2] E. Beutell and A. Kutzelnigg, Monatsh. Chem. **61**, 69 (1932).
[3] B. Andress and E. Mollwo, Naturwiss. **46**, 623 (1959).
[4] B. Andress, Z. Physik **170**, 1 (1962).
[5] D. G. Thomas, J. Phys. Chem. Solids **15**, 86 (1960). For a further discussion of the ZnO problem, especially with regard to symmetry, see the paper by J. J. Hopfield, *ibid.* **15**, 97 (1960).
[6] R. E. Deitz, J. J. Hopfield, and D. G. Thomas, J. Appl. Phys. Suppl. **32**, 2282 (1961).
[7] J. L. Birman, Phys. Rev. Letters **2**, 157 (1959); see also, J. L. Birman, Phys. Rev. **114**, 1490 (1959).

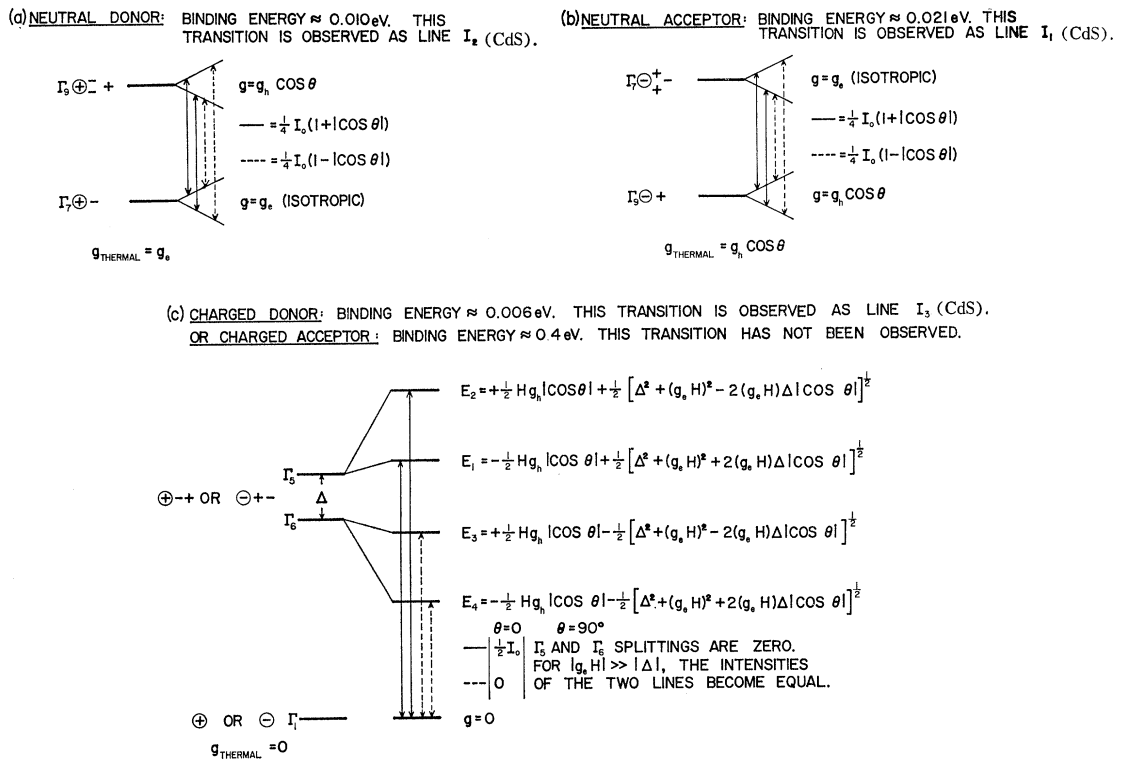

FIG. 2. A schematic representation of the energy levels of complexes which can be formed using holes only from the top valence band. In (a) and (b), linear splittings are observed, but in (c) the splittings are more complex and the energy levels are given. The expressions associated with the dashed or solid lines refer to the intensities of transitions. θ is the angle between the crystalline c axis and the direction of the magnetic field. (After Thomas and Hopfield.)

metries and optical selection rules, is shown in Fig. 1.

An inspection of Fig. 1 reveals that the top valence band (A band) is of Γ_9 symmetry, while the two lower valence bands (B and C bands) are each of Γ_7 symmetry. Similarly, the Γ_1 conduction-band symmetry goes over to a Γ_7 symmetry under the action of the double group (inclusion of spin). One further notes that a Γ_7-Γ_9 conduction-to-valence-band optical transition is allowed for light polarized only in the mode $\mathbf{E}\perp C$, while the Γ_7-Γ_7 transitions are allowed for both modes of polarization ($\mathbf{E}\perp C$ or $\mathbf{E}\|C$).

In 1960, Thomas[5] made a rather detailed study of the optical properties of ZnO near the onset of intrinsic absorption and interpreted the data in terms of the wurtzite band structure derived from Birman's model; however, a paradox concerning the band polarizations arose, and the usually observed wurtzite absorption dichroism was not straightforward. In fact, reflectivity measurements showed that the ground-state exciton transitions were polarized in the $\mathbf{E}\perp C$ mode for the two top valence bands, while the exciton transition from the third valence band appeared to be polarized in the mode $\mathbf{E}\|C$. Thomas also observed from absorption experiments[5] that transitions from the top valence band were at least partially polarized in the mode $\mathbf{E}\|C$. Based primarily on these polarization experiments, he concluded that the states of the first and third valence bands were mixed and that the two top valence bands were reversed in ZnO. This band reversal assigns a Γ_7 symmetry to the top valence band, a Γ_9 symmetry to the second band, and a Γ_7 symmetry to the third or lowest band.

The ZnO band-symmetry paradox has not been observed in the other wurtzite crystals from the II–VI group. For example, in a detailed study of the optical properties of CdS crystals near the absorption edge, Thomas and Hopfield[8,9] developed a theory from Birman's model that successfully explained their intrinsic exciton data. A similar theory was later successfully applied to the intrinsic exciton structure of CdSe by Wheeler and Dimmock[10] and, more recently, to ZnS by Wheeler and Miklosz.[11]

While the intrinsic- or free-exciton spectra are useful in studying the optical-band parameters of semiconductors, the corresponding bound-exciton-complex spec-

[8] D. G. Thomas and J. J. Hopfield, Phys. Rev. **116**, 573 (1959).
[9] J. J. Hopfield and D. G. Thomas, Phys. Rev. **122**, 35 (1961).
[10] R. G. Wheeler and J. O. Dimmock, Phys. Rev. **125**, 1805 (1962).
[11] R. G. Wheeler and J. C. Miklosz, *Proceedings of the International Conference on the Physics of Semiconductors* (Dunod Cie., Paris, 1964), p. 873.

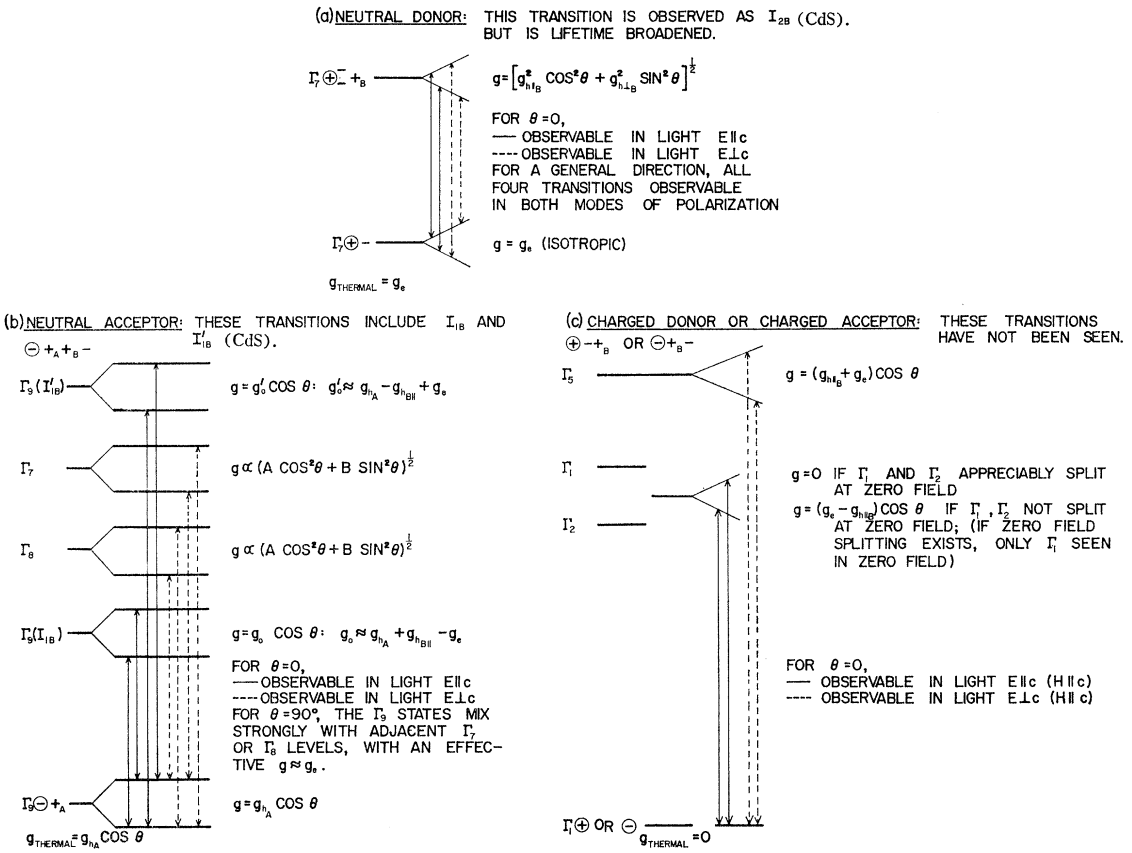

FIG. 3. A schematic representation of the energy levels of complexes which can be formed using holes from the second or B valence band, as well as from the top or A valence band. θ is the angle between the crystalline c axis and the direction of the magnetic field. (After Thomas and Hopfield.)

tra,[12] when examined in high magnetic fields at low temperature, are sometimes even more useful and have frequently proved to be a powerful tool in the analysis of the defect structure of such semiconductors as CdS. It is the principal purpose of this paper to report the observation of a series of sharp, bound-exciton spectral lines in ZnO, similar to those which have been previously observed in CdS,[13,14] and to interpret these lines in terms of a bound-exciton theory due to Thomas and Hopfield[13] and Hopfield.[15]

In their study of bound excitons in CdS, Thomas and Hopfield[13] have shown how the bound excitons should split in a magnetic field. The expected Zeeman splittings for bound excitons made up from holes in the top valence band (giving rise to a $\Gamma_7 \leftrightarrow \Gamma_9$ transition) are shown in Fig. 2; similarly, the splittings for corresponding exciton complexes formed from holes in the second valence band (giving rise to a $\Gamma_7 \leftrightarrow \Gamma_7$ transition) are shown in Fig. 3. An inspection of Figs. 2 and 3 reveals that, for appropriate orientations of the crystalline c axis in the magnetic field, there are significant differences between the Zeeman splittings for the $\Gamma_7 \leftrightarrow \Gamma_9$ and $\Gamma_7 \leftrightarrow \Gamma_7$ optical transitions. This expected difference in the Zeeman patterns suggested that a study of the Zeeman effects in bound excitons might prove helpful in examining the ZnO band-symmetry problem.

II. EXPERIMENTAL

The ZnO crystals used in these experiments were of the platelet type, varying in thickness from a few microns (3–5) up to about 50 μ, and were grown from the vapor phase in a vapor-transport reaction. Details of the crystal-growing technique will be published elsewhere. Most of the crystals used in the present measurements were grown in our laboratory; however, a few bulk-type samples were obtained from other sources: (1) The 3M Company (several

[12] As used here, "bound-exciton complex" refers to a free or intrinsic exciton (hydrogenically bound hole-electron pair) molecularly bound to a chemical defect, where the chemical defect can derive from either an impurity atom or a host-lattice defect and can assume the form of a neutral or ionized donor or acceptor in the semiconductor. The bound excitons are sometimes referred to as "impurity" excitons.

[13] D. G. Thomas and J. J. Hopfield, Phys. Rev. **128**, 2135 (1962). See also D. G. Thomas and J. J. Hopfield, Phys. Rev. Letters **7**, 316 (1961).

[14] D. C. Reynolds and C. W. Litton, Phys. Rev. **132**, 1023 (1963).

[15] J. J. Hopfield, Ref. 11, p. 725.

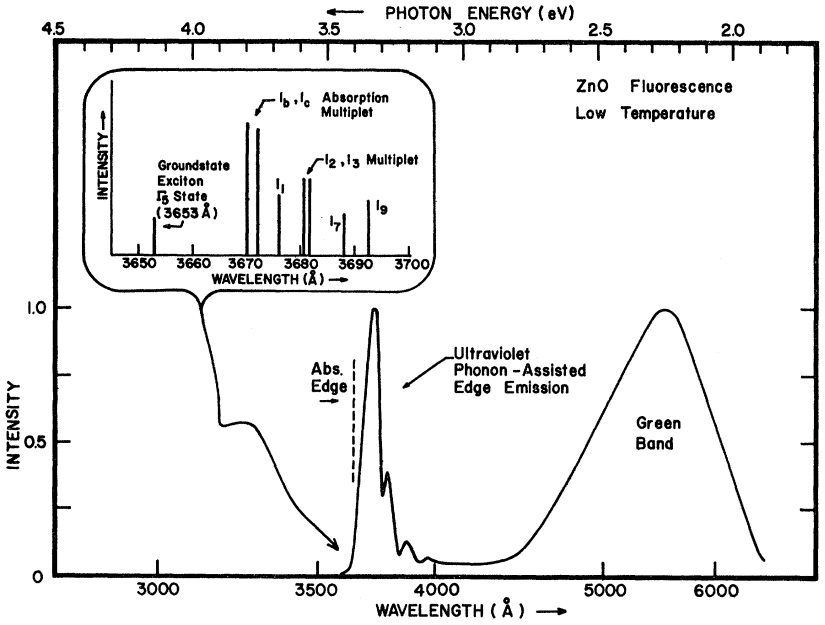

FIG. 4. A diagram of the ZnO fluorescence spectrum at low temperature. Shown in the spectrum is the well-known broad "green" band, as well as the characteristic, phonon-assisted edge emission which appears in the near ultraviolet and whose peaks are separated by the longitudinal-optical phonon energy, $\hbar\omega \approx 0.079$ eV. The inset diagram shows the highly resolved and detailed spectrum which appears between the absorption edge (ground-state exciton, Γ_5 state) and the phonon-assisted emission; this detailed spectrum is composed of many sharp lines, several of which form the basis of the present study. In the inset spectral diagram, lines are drawn to represent several of the fluorescence lines at the appropriate wavelength. While intensities are generally represented by line heights, intensities are not meant to be quantitatively comparable. The absorption multiplet, I_b, I_c (3669.66, 3671.9 Å), is drawn as two fluorescence lines for the sake of comparison. Andress (Ref. 4) previously studied the broad-band emission from ZnO and observed a spectral distribution similar to that shown in the diagram.

small "greenish" prisms and a few prismatic needles); (2) Litton Industries (several large hydrothermally grown samples); and (3) Aerospace Research Company (one big solution-grown crystal). The platelet-type crystal samples were mounted strain-free (glued lightly at one end) on a small brass sample holder that was, in turn, attached to one end of a long stainless-steel rod. The sample holder was then placed in the tip of a glass Dewar vessel containing liquid He; hence, the specimens were cooled by immersion and were maintained at the temperature of the refrigerant. In order to lower the temperature of the refrigerant, provision was made for pumping on the liquid He (high-speed vacuum pump), and temperatures were measured by means of vapor-pressure thermometry, using an oil manometer. All of the experiments reported here were performed at approximately 1.2°K. For the Zeeman effects measurements, the tip of the Dewar vessel was placed between the pole tips of a large, conventional electromagnet, capable of producing magnetic fields up to 45 000 G. The crystal fluorescence, excited from the crystals by light from a high-pressure Hg lamp with blacklight filter, was focused onto the slit of a Bausch and Lomb 2-m grating spectrograph. This spectrograph employed a large, 55 000 line/in., grating and produced a reciprocal dispersion of 2 Å/mm in first order. Spectral resolution was better than 0.05 Å. All of the spectra were photographically recorded on Kodak 103aO spectroscopic plates.

III. RESULTS AND DISCUSSION

A. The ZnO Spectrum

A total of ten rather prominent, sharp and narrow, edge-emission lines have been observed in ZnO spectra, most of which showed Zeeman effects, similar to the effects which were previously reported for CdS.[13,14] Equally sharp and narrow (line half-widths $\lesssim 0.1$ Å) were the eight absorption lines which were also observed over the same spectral range as the fluorescence lines; these lines appeared as the result of absorbing the exciting radiation as well as from the self-absorption of a continuum, background emission from the crystals. Most of the absorption lines also show Zeeman effects. In some cases, more than one line is observed to arise from a similar type of exciton complex (i.e., exciton bound to neutral donor, ionized donor, etc.); hence, in these cases, only the splitting of a representative line is discussed in the text, while other lines that arise from a similar complex are simply indicated.

Illustrated in Fig. 4 are the general features of the ZnO fluorescence spectrum, showing several peaks of the broad-band, phonon-assisted, edge emission (near ultraviolet) and the well-known broad green band which peaks at about 5500 Å. Several investigators[1,4]

TABLE I. A summary of the ZnO emission lines reported in the text. Temperature of 1.2°K at $H=0$.

Line	λ (Å)	Energy (eV)	$\bar{\nu}$ (cm^{-1})	Preferential polarization
I_1	3676.32	3.3720	27 201.1	$\mathbf{E}\parallel C$
I_2	3680.63	3.3680	27 169.3	$\mathbf{E}\perp C$
I_3	3681.59	3.3671	27 162.2	$\mathbf{E}\parallel C$
I_4	3687.12	3.3621	27 121.4	$\mathbf{E}\perp C$
I_5	3687.54	3.3617	27 118.3	$\mathbf{E}\perp C$
I_6	3688.40	3.3609	27 112.0	$\mathbf{E}\perp C$
I_7	3689.03	3.3604	27 107.4	$\mathbf{E}\perp C$
I_8	3689.26	3.3601	27 105.7	$\mathbf{E}\perp C$
I_9	3692.64	3.3571	27 080.9	$\mathbf{E}\perp C$
I_{10}	3696.50	3.3536	27 052.6	$\mathbf{E}\perp C$

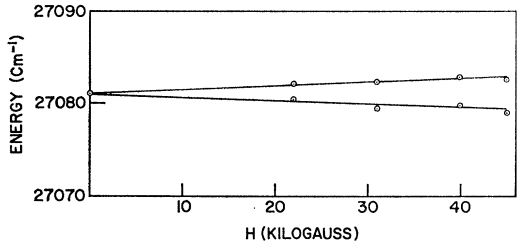

FIG. 5. Splitting of the emission line I_9 (3692.64 Å) as a function of magnetic field strength at 1.2°K for the orientation $C \perp H$.

have studied the phonon-assisted peaks as well as the broad green peak in ZnO, and it has been shown that the relative intensities of these two peaks depend markedly on the electrical conductivity of the crystals, with the intensities of the two peaks becoming nearly equal at reasonably high conductivities; it has also been shown that the conductivity of ZnO is affected strongly by excess Zn in the crystals and that the conductivity increases rapidly with increasing Zn concentration. In the crystals used in the present experiments, the fluorescent intensities in both the ultraviolet and the green were rather strong, yet crystal resistivities were quite high, as determined from photoconductivity measurements[16] with the same crystals. In addition to the platelets, we have also examined the edge fluorescence of several pale-green prism-type ZnO crystals, whose resistivities were quite low ($\rho \lesssim 1\Omega$ cm); however, the emission from these crystals, while fairly strong in both the uv and the green, was not characterized by the fluorescent line spectra of bound excitons. Also shown in Fig. 4 (inset diagram) is the highly resolved, "blown-up" picture of the spectral region between the absorption edge (A-exciton ground state[5,17]) and the first peak ($N=0$) of the phonon-assisted edge emission. It is this region of the spectrum that is of greatest interest here, since it contains the bound exciton lines (emission and absorption). These exciton complex lines, a few of which are pictured in the spectrum, are observable only in high-resolution spectra at low temperature. The emission and absorption lines are summarized in Tables I and II, respectively. In addition to the lines listed in the tables, some sharp, relatively weak, lines were observed at somewhat longer wavelengths; however, these lines are not discussed in the present work.

B. Emission Line I_9

The emission line I_9 undergoes a linear splitting in a magnetic field. Plotted in Fig. 5 is the splitting of the I_9 line (photon energies of its split components in units of cm^{-1}) as a function of magnetic field strength with the crystalline c axis oriented perpendicular to the direction of the magnetic field ($C \perp \mathbf{H}$); as can be seen from the figure, I_9 splits into a doublet. In terms of the Thomas-Hopfield theory of bound excitons,[13] one would expect a doublet splitting (with $C \perp \mathbf{H}$) to arise from an exciton bound to a neutral donor or acceptor site in a $\Gamma_7 \leftrightarrow \Gamma_9$ optical transition, as shown in Fig. 2. In order to further test the theory as applied to the I_9 line, the Zeeman splitting of I_9 was examined, i.e., the line splitting was measured as a function of the crystal orientation (orientation of the c axis with respect to the magnetic field direction) in a constant magnetic field whose intensity was maintained at 45 000 G. The Zeeman splitting of I_9 is shown in Fig. 6. From the figure, it is obvious that I_9 splits into a quartet for all orientations except $C \perp \mathbf{H}$ ($\theta = 90°$). Somewhat less obvious, however, is the fact that the high- and low-energy components of the quartet are not observed in the orientation $C \| \mathbf{H} (\theta = 0°)$; these lines are missing because the transitions are not allowed by spin consideration. It was also observed that each of the four split components of I_9 were polarized in the mode $\mathbf{E} \perp C$. In fact, all of the measurements concerning this line (especially the Zeeman splittings) tend to suggest that it arises from a bound exciton complex of the neutral donor or acceptor type.

When emission and absorption lines, arising from bound exciton complexes, undergo linear Zeeman splittings, Thomas and Hopfield have shown[13] that the hole and electron g values for such splittings obey the relation

$$g = g_e \pm g_h = g_{e0} \pm g_{h\parallel} \cos\theta, \qquad (1)$$

where g_e and g_h are electron and hole g values, respectively; g_{e0} is the isotropic g value of the electron; $g_{h\parallel}$ is the g value of the hole when $C \| \mathbf{H}$; and θ is, as usual, the angle between the c axis and the direction of H. Equation (1), implicit in Figs. 2(a) and (b), implies, in the linearly split quartet of Fig. 6, that the outer pair of lines (high- and low-energy) splits as the sum of the g values ($g_e + g_h$), and that the inner pair of lines splits as the difference of the g values ($g_e - g_h$). Remembering that the hole in a neutral donor or acceptor complex is not spin-split when the crystal is oriented

TABLE II. A summary of the ZnO absorption lines reported in the text. Temperature of 1.2°K at $H=0$. Some of the absorption lines were observed as the self-absorption of a continuum emission from the crystals.

Line	λ (Å)	Energy (eV)	$\bar{\nu}$ (cm^{-1})	Preferential polarization
I_a	3666.31	3.3812	27 275.5	$\mathbf{E} \| C$
I_b	3669.66	3.3781	27 250.5	$\mathbf{E} \perp C$
I_c	3671.99	3.3760	27 233.2	$\mathbf{E} \| C$
I_d	3682.61	3.3662	27 154.6	$\mathbf{E} \perp C$
I_e	3683.33	3.3655	27 149.3	$\mathbf{E} \perp C$
I_f	3684.07	3.3649	27 143.9	$\mathbf{E} \perp C$
I_g	3690.22	3.3593	27 098.6	$\mathbf{E} \perp C$
I_h	3694.93	3.3550	27 064.1	$\mathbf{E} \| C$

[16] Y. S. Park (private communication).
[17] Y. S. Park, D. C. Reynolds, C. W. Litton, and T. C. Collins (to be published).

with $C\perp\mathbf{H}$, we can calculate an electron g value from the usual relation $\Delta E=g\beta H$, where β is the Bohr magneton. Hence, from the data of Fig. 5, we calculate an electron g value of -1.9_3 for I_9. Recalling that the inner pair of lines in Fig. 6 splits as $g_e-g_h=\Delta E/\beta H$, we find $g_e-g_h=0.69$, using ΔE at the orientation $C\|\mathbf{H}$; hence, the g value for the hole of the I_9 complex is calculated to be $g_h=-1.93+0.69=-1.24$. Thermalization effects were not observed in the split components of I_9. One would not expect to observe thermalization effects in the fluorescence from an exciton bound to a neutral donor site; on the other hand, this complex is not the only possibility in the present case. It is sometimes possible to observe thermalization effects in the emission from an exciton bound to a neutral acceptor site when the crystal is oriented with $C\perp\mathbf{H}$; however, the observation of emission-line thermalization, in this case, requires that the exciton lifetime in the upper state be long enough for thermalization of the electron spins to occur. For example, consider the neutral acceptor complex of Fig. 2 (b) in the orientation $C\perp\mathbf{H}$, where the upper state $\ominus_+{}^+-$ is electron spin-split into a doublet, while the lower state $\ominus+$ is not split, since hole splitting is not allowed. Now, if the complex is sufficiently long lived in its upper state, the electron spins can thermalize with either increasing magnetic field or decreasing temperature, so that the lower energy component of the spin splitting will become more densely populated, giving rise to a low-energy emission line that is more intense than its high-energy counterpart. Hence, the I_9 line might arise from a neutral acceptor complex and still not show thermalization effects as a consequence of a short-lived upper state. Interestingly, in CdS, thermalization has been observed in the magnetically split components of the 4888-Å emission line,[14] a line which has been attributed to a neutral acceptor complex.[13] In the case of I_9, a lack of knowledge of the exciton complex lifetime in the upper state precludes the possibility of distinguishing between a neutral donor and a neutral acceptor complex. The lines I_6, I_7, and I_8 have also been examined and have been found to be of the same type as line I_9, i.e., they are derived from an exciton bound either to a neutral donor or a neutral acceptor.

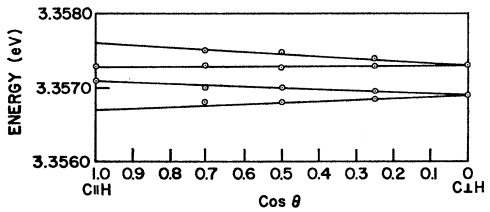

FIG. 6. Splitting of the I_9 emission line as a function of $\cos\theta$ in a constant field of 45 000 G at 1.2°K. Here, as in subsequent plots, θ is the angle between the crystalline c axis and the direction of the magnetic field. Note that this line splits as a doublet for the orientation $\theta=0°$ and $\theta=90°$, while for intermediate orientations, $0°<\theta<90°$, quartets are observed.

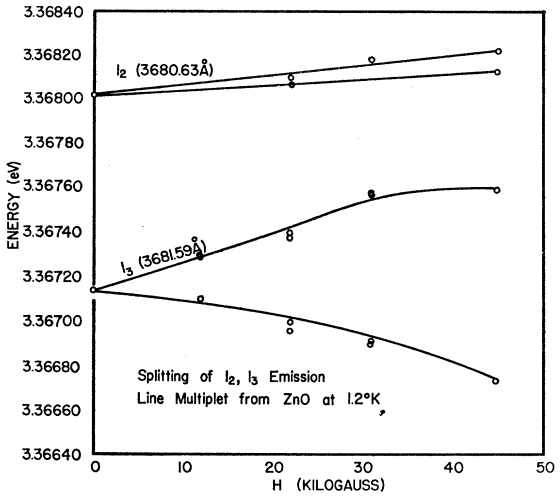

FIG. 7. Splitting of the I_2, I_3 (3680.63, 3681.59 Å) emission line multiplet as a function of magnetic field strength at 1.2°K. The crystal is oriented with $C\|\mathbf{H}$. Note the zero-field splitting at $H=0$. Also note the nonlinear splitting of the I_3 component. The I_2 component is split but not resolved at the lower fields.

C. Emission Line Multiplet, I_2–I_3

The emission line multiplet I_2-I_3 is a zero-field split pair, as is revealed in the line splittings of Fig. 7, where the splittings of the high-energy component I_2 (3681.59 Å) are plotted as a function of magnetic field strength with the crystal oriented at $C\|\mathbf{H}$. A zero-field splitting of 9.0×10^{-4} eV is measured, and a nonlinear splitting is indicated for the I_3 component. According to the observations of Thomas and Hopfield,[13] the zero-field splitting of the multiplet suggests a bound exciton complex composed of an intrinsic exciton molecularly bound to an ionized center; moreover, the small exciton-to-center binding energy (approximately 0.02 eV) makes it likely that the center is an ionized donor. As Thomas and Hopfield have shown,[13] it can be argued that such a zero-field splitting of lines arises from a hole-electron, spin-spin exchange interaction in the upper state [see Fig. 2(c)].

The Zeeman splitting of the I_2-I_3 complex has been measured and is shown in Fig. 8, where the magnetic splittings of the two components (I_2 and I_3, circled points) have been plotted as a function of orientation of the crystalline c axis with respect to the magnetic field direction ($\cos\theta$) while the field intensity was held constant at 45 000 G. A comparison of the data of Figs. 7 and 8 with the fourfold splitting scheme of Fig. 2(c) reveals that the I_3 line of the multiplet (low-energy component) corresponds to a transition from the Γ_6 exciton state,[18] and we have observed that

[18] Here, the expression "Γ_6 exciton" (or "Γ_5 exciton") alludes to bound-exciton states; in particular, it refers to ionized complex states formed from the binding of an intrinsic exciton to an ionized donor or acceptor, where the intrinsic exciton can be in either a Γ_5 or a Γ_6 state. We recall that an intrinsic exciton in a Γ_6 state is one whose hole and electron spins are parallel, while the spins are antiparallel for an exciton in the Γ_5 state.

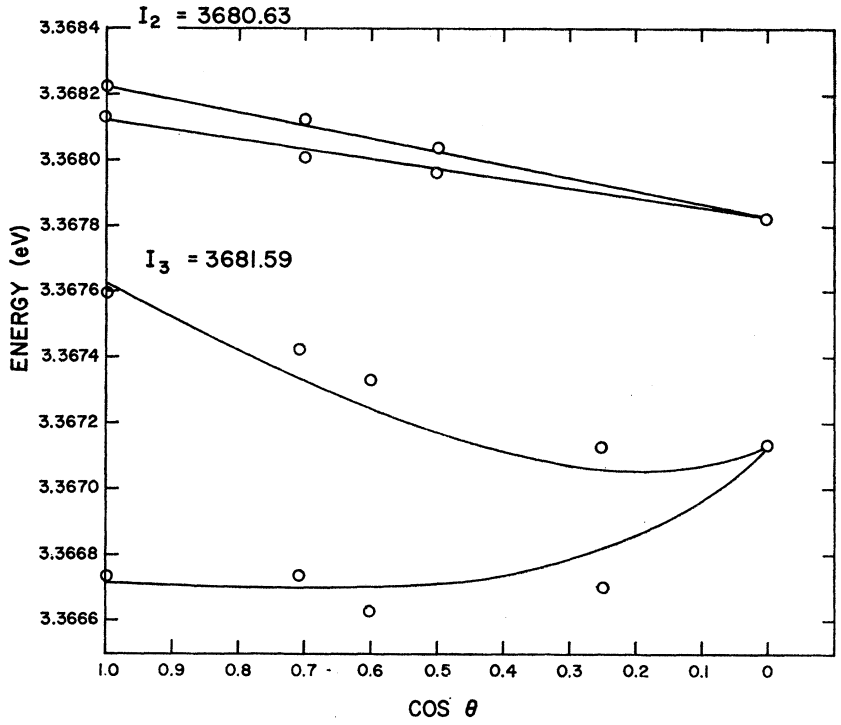

FIG. 8. Splitting of the I_2, I_3 (3680.63, 3681.59 Å) emission line multiplet at 1.2°K as a function of $\cos\theta$ in a constant magnetic field of 45 000 G. The circular points represent the experimentally determined splittings for both components (I_2 and I_3), while the solid curves are a plot of theoretical splittings determined from the expressions of Fig. 2 (ionized complex). When the crystal assumes the orientation $C\perp H$ ($\cos\theta=0$), note that neither I_2 nor I_3 split at maximum field.

the I_3 line is polarized in the mode $\mathbf{E}\|C$, as expected for a Γ_6 exciton transition; similarly, the I_2 component of the multiplet corresponds to a Γ_5 exciton transition and is polarized in the mode $\mathbf{E}\perp C$, as expected. In the orientation $C\|\mathbf{H}$ ($\cos\theta=1$), the I_3 or Γ_6 component splits as the sum of the g values (g_e+g_h), whereas the I_2 or Γ_5 component splits as the difference of the g values (g_e-g_h), as shown by the large splitting for I_3 and the small splitting for I_2 in Fig. 8. In fact, on the basis of predicted splittings and polarizations for an ionized complex in a $\Gamma_7\leftrightarrow\Gamma_9$ optical transition, as shown in Fig. 2(c), one may reasonably conclude that the I_2-I_3 multiplet conforms to the specification of an exciton bound to an ionized donor or acceptor. Using the value of zero-field splitting quoted above ($\Delta=9.0\times10^4$ eV) and a least-squares fit to the experimental splittings of Fig. 8 (circled points), the energy level expressions in Fig. 2(c) (i.e., the levels E_1, E_2, E_3, and E_4) are plotted as the solid curves in Fig. 8. Rather good agreement (excellent for the I_2 component) is obtained between the calculated and experimental splittings of the I_2-I_3 complex; moreover, from these "weighted" line splittings, the following g values are obtained, $g_e=1.9_5$ and $g_h=1.5_1$. Of the several emission lines listed in Table I, the line I_1 also appears to arise from an ionized exciton complex; however, the intensities of its split components are too weak to permit a meaningful study in terms of the ionized complex model.

D. Absorption Line Multiplet, I_b–I_c

As is pointed out above (Sec. A), absorption spectra containing many sharp lines are often observed in selected ZnO crystals, primarily as a self-absorption of continuum fluorescence from the crystals. The most intense absorption line in these spectra is the line I_b (3669.66 Å); also, associated with this line is another weaker line which we have labeled I_c (3671.99 Å). Hence, as we shall show in the present measurements, the two absorption lines appear as a zero-field-split pair and form the absorption multiplet, I_b-I_c. Thomas has previously observed these two lines and has labeled the line I_b as line A and the line I_c as line A_m; however, he has interpreted the line I_b as an intrinsic exciton line, arising from the Γ_5 ground state of the A exciton (i.e., the ground-state exciton from the top valence band). Thomas has also examined the line I_c, but, like I_b, he has interpreted this line as an intrinsic exciton line, arising, in this case, from an exciton in the Γ_1 state and of top valence-band origin. It is interesting that, if the Γ_1 exciton assignment is to hold for the line I_c, the exciton symmetry arguments require, in general, that the top valence band be of

TABLE III. Intrinsic exciton symmetries for the three valence bands of the wurtzite structure (ground state only). It is understood that there is a conduction band of Γ_7 symmetry associated with each of the excitons.

Exciton	Valence-band symmetry	Exciton symmetry (ground state)
A	Γ_9	$\Gamma_5+\Gamma_6$
B	Γ_7	$\Gamma_1+\Gamma_2+\Gamma_5$
C	Γ_7	$\Gamma_1+\Gamma_2+\Gamma_5$

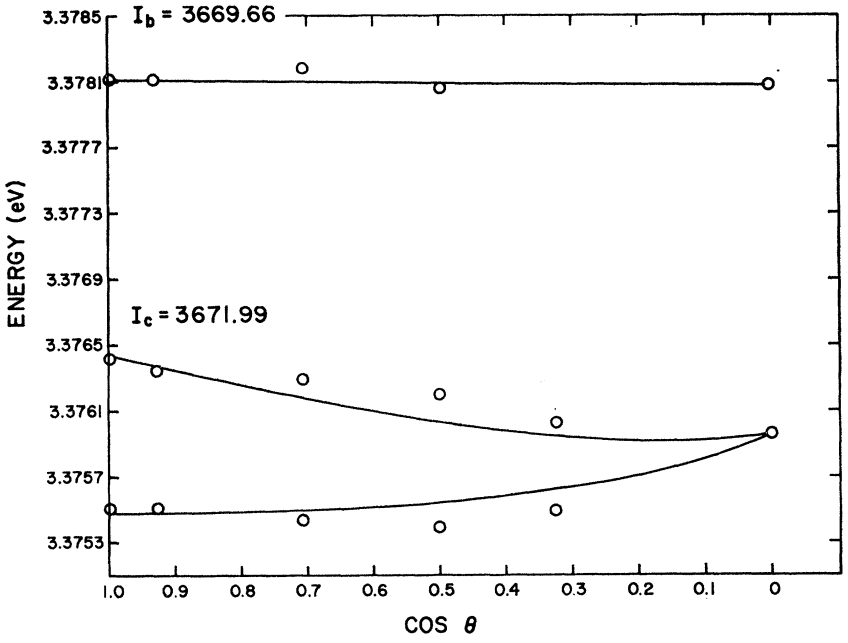

FIG. 9. Splitting of the I_c, I_b (3689.66, 3671.99 Å) absorption multiplet at 1.2°K as a function of cosθ in a constant field of 45 000 G. As in Fig. 8, the data points represent experimental energies and splittings, while the solid curves are the calculated splittings (calculated from the energy level expressions of Fig. 2). The I_b component does not appear to split.

Γ_7 symmetry, as shown in Table III. This assertion regarding valence-band symmetry does not consider strong "valence-band mixing" as a possibility, since such "mixing" has not been unambiguously demonstrated for excitons in the wurtzite structure.

We have examined the splitting of the absorption-line multiplet I_b-I_c in a magnetic field. The experimentally determined Zeeman splittings are shown in Fig. 9 (circled data points), where, as usual, the line splittings are plotted as a function of crystal orientation (splitting versus cosθ) in a magnetic field of constant field strength. As can be seen from Fig. 9, the I_c component of the multiplet shows a large splitting in the orientation $C\|\mathbf{H}$ (cosθ=1); also, this line is polarized in the mode $E\|C$. The polarization and splitting of I_c suggest that this line derives from a Γ_6 exciton state, in direct analogy to the I_3 component of the emission line multiplet, I_2-I_3, which is shown to arise from an ionized donor or acceptor complex (see Sec. C). If we treat the absorption line multiplet I_b-I_c as arising from a bound-exciton complex, in which the chemical center is ionized, we can again calculate the expected splittings for such a complex from the energy-level expressions (E_1, E_2, E_3, and E_4) of Fig. 2(c). Substituting a measured value of zero-field splitting, $\Delta=2\times10^{-3}$ eV, into the expressions of Fig. 2(c), the following electron and hole g values were obtained from a least-squares fit of the equations to the experimental data: $g_e=1.9_5$ and $g_h=1.7_4$. Using these parameters in the equations of Fig. 2(c), we have calculated the Zeeman splittings for the I_b-I_c multiplet. These splittings are plotted as the solid curves in Fig. 9. The line I_b is the high-energy component of the multiplet and corresponds to the Γ_5 exciton transition, the splitting of which is proportional to the difference between the electron and hole g values (g_e-g_h). Since the I_b components splits as the difference between g values and since the electron and hole g values are of nearly the same magnitude in the complex (1.9_5 as compared to 1.7_4), the expected splitting for I_b is rather small. This prediction is born out experimentally, since a splitting is not observed for the I_b components, as shown in Fig. 9. The circular data points represent the measured energies of the I_b line at the various orientations, and the single solid line drawn through these points represents the calculated splitting of I_b. As shown in Fig. 9, the experimental splitting of the I_c component at the intermediate angles ($0°\leq\theta\leq90°$) are somewhat larger than that predicted by theory; however, a similar trend (deviation) is also observed for the I_3 component of the emission-line multiplet, I_2-I_3. In spite of small deviations, there is good agreement between the experimental data and the general features of the theoretical model.

IV. CONCLUSIONS

In the present work, a systematic study has been made of the sharp, narrow, emission and absorption lines which occur at low temperature in the extrinsic spectral region of ZnO, near the onset of the intrinsic absorption; moreover, it has been shown that these lines arise from bound-exciton complexes and that they can be assigned, on the basis of Zeeman splitting measurements, to neutral or ionized exciton complexes. In fact, all of the Zeeman effects for bound-exciton complexes in ZnO are quite similar to the corresponding effects previously reported for CdS,[13–15] and we have shown that the bound-exciton complex theory[13] for

TABLE IV. Typical bound-exciton parameters for several of the ZnO lines reported in the text.

Line	Type of Zeeman splitting	Exciton complex	Energy below Γ_9 exciton	g_e (g value of electron) $C\|\|\mathbf{H}$	g_e (g value of electron) $C\perp\mathbf{H}$	g_h (g value of hole) $C\|\|\mathbf{H}$	g_h (g value of hole) $C\perp\mathbf{H}$
I_9	linear	neutral donor or acceptor	0.036	−1.93	−1.93	−1.24	0
I_2-I_3	nonlinear zero-field split	ionized donor or acceptor	0.025	−1.94	−1.94	−1.51	0
I_b-I_c	nonlinear zero-field split		0.015	−1.95	−1.95	−1.74	0

CdS fits the ZnO Zeeman data quite well. As in CdS, the ZnO exciton complex lines showed both linear and nonlinear Zeeman splittings, as well as zero-field-split pairs, orientation-dependent g values for holes, isotropic electron g values, polarizations and symmetries dependent upon the energy bands from which the intrinsic exciton was derived, etc. Typical exciton complex data, deduced from Zeeman effects, are summarized in Table IV for the several ZnO lines discussed in the text.

As can be seen from the three line complexes of Table IV, the g value of the electron, g_e, is isotropic (same for both $C\|\mathbf{H}$ and $C\perp\mathbf{H}$) and is essentially insensitive to the state of binding of the exciton, as g_e is nearly of the same magnitude in the three different complexes; on the other hand, the hole g value g_h, ranging from 0 at $C\perp\mathbf{H}$ to a maximum value at $C\|\mathbf{H}$, is not only anisotropic, but also quite sensitive to the state of binding of the intrinsic exciton in the complex, as expected from the Thomas-Hopfield model[13] (note the different values of g_h in the different complexes when the crystal is oriented to $C\|\mathbf{H}$). Several of the more than 20 emission and absorption lines examined in the present study (18 of which are listed in Tables I and II) were linearly split lines which arose from neutral complexes, but thermalization effects could not be demonstrated conclusively in the split components of these lines; consequently, it was not possible to determine, in the usual way, whether the neutral complex was of donor or acceptor origin.

If one uses the line assignments as given by Thomas,[5] a spin-orbit interaction parameter is obtained which has the magnitude and negative sign (different from all other II–VI compounds) to cancel the coefficient of the P_z term in the top Γ_7 valence-band wave function; hence,

$$\psi_{\Gamma_7} \propto (P_x \pm iP_y) + (2-\delta/E)P_z,$$

where $(2-\delta/E)\approx 0$, δ is the spin-orbit parameter and E is the energy difference between the Γ_9 and Γ_7 valence bands. This has the effect that both Γ_7 and Γ_9 have hole g values given by $g_h = g_{h\parallel}\cos\theta$, and the Zeeman effects of both would follow those given for the Γ_7-Γ_9 transitions given in Fig. 2. Thus no definite conclusion as to the band symmetry can be made without further study. However, an important point is that the relative intensities and polarizations of the neutral centers fit the Γ_7-Γ_9 transitions, and the relative intensities are determined by the symmetries, as one can see by invoking the Wigner-Eckart theorem.[19]

ACKNOWLEDGMENTS

The authors express their appreciation to Dr. R. Euwema for his assistance in writing programs for the 7090 IBM computer.

[19] See, e.g., A. R. Edmonds, *Angular Momentum in Quantum Mechanics* (Princeton University Press, Princeton, New Jersey, 1957), p. 4. See also K. W. McVoy, Rev. Mod. Phys. 37, 84 (1965).